Carbon-Doped MgB_2 Thin Films Grown by Hybrid Physical-Chemical Vapor Deposition

A. V. Pogrebnyakov, J. M. Redwing, J. E. Giencke, C. B. Eom, V. Vaithyanathan, D. G. Schlom, A. Soukiassian, S. B. Mi, C. L. Jia, J. Chen, Y. F. Hu, Y. Cui, Qi Li, and X. X. Xi

***Abstract*—Carbon-doped MgB_2 thin films have been produced with hybrid physical-chemical vapor deposition (HPCVD) by adding a carbon-containing metalorganic magnesium precursor, bis(methylcyclopentadienyl)magnesium, to the carrier gas. The amount of the carbon added, thus the carbon content in the films, was controlled by the flow rate of a secondary hydrogen gas flow through the precursor bubbler. X-ray diffraction and electron microscopy showed that the carbon-doped MgB_2 films are textured with c-axis oriented columnar nano-grains and highly resistive amorphous areas at the grain boundaries. When the amount of carbon in the films increases, the resistivity increases dramatically while T_c decreases much more slowly as the current-carrying cross section is reduced by the grain boundaries. The temperature-dependent part of the resistivity, $\Delta\rho \equiv \rho(300\ \mathrm{K}) - \rho(50\ \mathrm{K})$, increases only modestly until the highly resistive grain boundaries completely cut off the conducting path. The impact of the reduced cross section on critical current density J_c is discussed.**

***Index Terms*—Carbon doping, hybrid physical-chemical vapor deposition, magnesium diboride, thin films.**

I. Introduction

ONE of the critical material parameters for the application of the 39-K superconductor MgB_2 to generate high magnetic fields is a high upper critical field H_{c2} [1]. Clean MgB_2 samples show low upper critical fields [2]. In high-resistivity MgB_2 films H_{c2} can be much higher [1]. Because of the multiple impurity scattering channels and the two-gap nature of superconductivity in MgB_2 [3]–[5], H_{c2} can be enhanced well above the estimate $H_{c2}(0) = 0.69T_cH'_{c2}(T_c)$ from the one-gap theory. It has been recently shown that carbon doping can substantially enhance H_{c2} of MgB_2 [6], [7]. Using a hybrid physical-chemical vapor deposition (HPCVD) technique, which produces very clean in situ epitaxial MgB_2 films [8], we have deposited carbon doped MgB_2 films by adding carbon-containing Mg precursor to the carrier gas [9]. The $H_{c2}(0)$ of such carbon-doped films in the parallel field is as high as $\sim$70 T [7]. In our previous publication [9] the structural and superconducting properties were discussed. In this paper, we present further details of the chemical and structural characterizations of the carbon-doped MgB_2 films as well as an in-depth discussion of their transport properties.

Manuscript received October 3, 2004. The work of X. X. Xi was supported by the Office of Naval Research (ONR) under Grant N00014-00-1-0294 and by the National Science Foundation (NSF) under Grant DMR-0306746 and Grant DMR-0103354. The work of J. M. Redwing was supported by the ONR under Grant N0014-01-1-0006 and by the NSF under Grant DMR-0306746. The work of C. B. Eom was supported by the MRSEC for Nanostructure Materials at the University of Wisconsin. The work of D. G. Schlom was supported by the NSF under Grant DMR-0103354 and the U.S. Department of Energy under Grant DE-FG02-03ER46063. The work Q. Li was supported by the NSF under Grant DMR-0405502.

A. V. Pogrebnyakov and X. X. Xi are with the Department of Physics and Department of Materials Science and Engineering, The Pennsylvania State University, University Park, PA 16802 USA (e-mail: avp11@psu.edu).

J. M. Redwing, V. Vaithyanathan, D. G. Schlom, and A. Soukiassian are with the Department of Materials Science and Engineering, The Pennsylvania State University, University Park, PA 16802 USA.

J. E. Giencke and C. B. Eom are with the Department of Materials Science and Engineering and Applied Superconductivity Center, University of Wisconsin, Madison, WI 53706 USA.

S. B. Mi and C. L. Jia are with the Institut für Festkörperforschung, Forschungszentrum Jülich GmbH, D-52425 Jülich, Germany.

J. Chen, Y. F. Hu, Y. Cui, and Q. Li are with the Department of Physics, The Pennsylvania State University, University Park, PA 16802 USA.

Digital Object Identifier 10.1109/TASC.2005.848871

II. Controlled Carbon Doping

The carbon-doped MgB_2 films reported in this paper were grown in situ by the HPCVD technique [10]. The films were deposited on (0001) 4H-SiC substrates at 720°C. The thickness of the films was around 2000 Å. In the standard HPCVD deposition, because of the highly reducing H_2 ambient during the deposition and the high purity sources of Mg and B (from B_2H_6), very clean MgB_2 thin films are produced with a residual resistivity above T_c as low as 0.26 $\mu\Omega$cm [8]. For carbon doping, we added bis(methylcyclopentadienyl)magnesium ($(MeCp)_2Mg$), a metalorganic magnesium precursor, to the H_2 carrier gas. A secondary hydrogen flow was passed through the $(MeCp)_2Mg$ bubbler which was held at 760 Torr and 21.6°C. Under such conditions $(MeCp)_2Mg$ is in the liquid form, and no additional heating of the transfer line is necessary. The secondary hydrogen flow, which contained $(MeCp)_2Mg$, was combined with the primary hydrogen flow in the reactor to a total of 700 sccm hydrogen flow. The flow of the boron precursor gas, 1% diborane (B_2H_6) in H_2, was kept at 15 sccm. The amount of carbon doping depends on the flow rate of the secondary hydrogen gas flow through the $(MeCp)_2Mg$ bubbler, $FR_{bubbler}$, which was varied between 25 and 200 sccm to vary the flow rate of $(MeCp)_2Mg$ into the reactor from 0.0065 to 0.052 sccm. The total pressure in the reactor during the deposition was 100 Torr.

While the carbon concentration in the films can be controlled easily by the secondary hydrogen flow rates through the $(MeCp)_2Mg$ bubbler, we did not measure the carbon concentrations for each films. Rather, a correlation between the carbon concentration and $FR_{bubbler}$ was established, from which the carbon concentration for each film was derived. The chemical compositions of a series of carbon-doped MgB_2 films were measured by wavelength dispersive X-ray spectroscopy (WDS). The result is plotted in Fig. 1, and the line

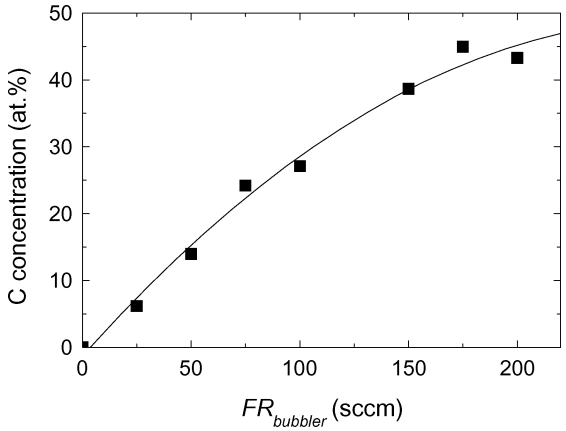

Fig. 1. Carbon content in the doped $\mathrm{MgB_2}$ films, determined by WDS, in the unit of the atomic percentage, as a function of the $\mathrm{H_2}$ flow rate through the $(\mathrm{MeCp})_2\mathrm{Mg}$ bubbler, $FR_{bubbler}$. The line is a polynomial fit with a standard deviatin of 2 at.%.

is a polynomial fit of the dependence of the carbon concentration on $FR_{bubbler}$ with a standard deviatin of 2 at.%. The scale of the carbon concentrations here is much higher than those in carbon-doped $\mathrm{Mg(B_{1-x}C_x)_2}$ single crystals [11] and filaments [6]. From the discussions below it is clear that only a small portion of the carbon in the films is doped into the $\mathrm{MgB_2}$ structure. The carbon concentrations determined by WDS result from carbon both in the $\mathrm{Mg(B_{1-x}C_x)_2}$ grains and in the grain boundaries. Although it is difficult to learn the exact carbon concentrations in the $\mathrm{Mg(B_{1-x}C_x)_2}$ grains, the nominal atomic concentrations determined by WDS can be used as a good indicator of the properties of the carbon-doped $\mathrm{MgB_2}$ films produced by the HPCVD technique described here. Using the correlation shown in Fig. 1, for example, for a film made with $FR_{bubbler} = 125$ sccm, we will use 34 at.% as its nominal carbon concentration.

III. Structure of Carbon-Doped Films

We have shown previously by cross-sectional transmission electron microscopy (TEM) that the carbon-doped $\mathrm{MgB_2}$ films have a granular structure [9]. They consist of columnar nano-grains of $\mathrm{Mg(B_{1-x}C_x)_2}$ with a preferential c-axis orientation and an equiaxial in-plane morphology, and an amorphous phase between the grains. Combined with the transport and superconducting properties of these films, we concluded that most likely a small portion of carbon is doped into $\mathrm{MgB_2}$ and the rest is contained in the amorphous grain boundaries. The films were further characterized using a four-circle x-ray diffractometer equipped with both 2-dimensional area detector and four-bounce monochromator. The $\theta - 2\theta$ scans show that the $\mathrm{MgB_2}$ $00l$ peaks are suppressed gradually as carbon concentration increases, and dramatically when the carbon concentration is above ~30 at.%. Both the c and a axes expand until about 30 at.%, above which the c lattice constant decreases and the a lattice constant increases dramatically. The doping dependence of the lattice constants is qualitatively different from those in carbon-doped single crystals and filaments, where the a axis lattice constant decreases but that of c axis remains almost constant for all the carbon concentrations [6], [11]. The difference may be due to the specific microstructures or the strain of the carbon-doped films. It may also be a critical factor to the much higher H_{c2} values observed in such films than in the bulk carbon-doped single crystals and filaments [7].

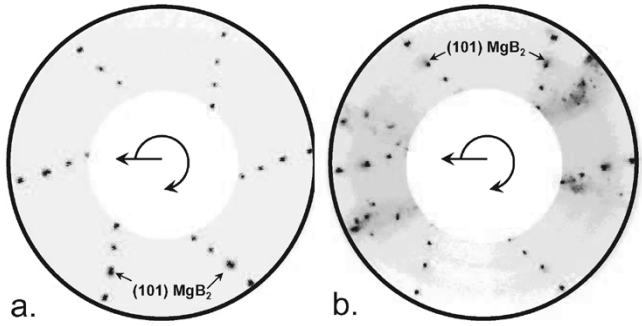

Fig. 2. X-ray diffraction pole figure of (a) an undoped $\mathrm{MgB_2}$ film, and (b) a carbon-doped $\mathrm{MgB_2}$ film with a nominal carbon concentration of 29 at.%.

The use of the 2-dimensional area detector, which is capable of capturing a large slice of the Ewald Sphere at constant ϕ, resulting in an image with axes of 2θ and χ, allows the detection of the impurity phases. These secondary phases are commonly missed in conventional point detector scans, but can easily be identified in this analysis due to the detector's wide detection angle and extreme sensitivity. The intensity of the individual image in the $2\theta/\chi$ scans are then integrated in χ and combined with images taken at different ϕ angles to produce the pole figures shown in Fig. 2. The first image (Fig. 2(a)) shows an undoped epitaxial film on a 0001 oriented SiC substrate. The peaks following a pin-wheel pattern are of $10l$ SiC. The $\mathrm{MgB_2}$ 101 reflections can be seen adjacent to the SiC 104 peaks. Fig. 2(b) is from a carbon-doped $\mathrm{MgB_2}$ film with a nominal carbon concentration of 29 at.%., which shows peaks from the secondary phases. The $\mathrm{MgB_2}$ peaks exhibited the same six-fold symmetry and texture with respect to χ as the undoped films, but were slightly dimmer. We attempted to identify the impurity phases by cross-referencing the d-spacings of the peaks with the χ and ϕ values at which they appear. Although a definitive identification was not possible, we concluded that they are most likely $\mathrm{B_4C}$, $\mathrm{B_8C}$, or $\mathrm{B_{13}C_2}$. The four-fold symmetric axis of the phase, which is clearly shown in the pole figure, is not collinear with the c-axis of the film. We cannot conclude from the x-ray analysis whether the phase exists within the boundary regions or it is incorporated into the $\mathrm{MgB_2}$ grains.

IV. Carbon Doping and Connectivity

The resistivity (in log scale) versus temperature curves for $\mathrm{MgB_2}$ films with different carbon doping levels are shown in Fig. 3(a). The resistivity increases dramatically with carbon doping, but the T_c of the film is suppressed much more slowly. For example, with a carbon concentration of 24 at.%, the residual resistivity increases from the undoped value of less than 1 $\mu\Omega$cm to ~ 200 $\mu\Omega$cm, but T_c only decreases from over 41 K to 35 K. The dependence of the transport and superconducting properties on carbon concentration is very different from those in carbon-doped single crystals [11] and filaments [6]. In carbon-doped single crystals, T_c is suppressed to 2.5 K

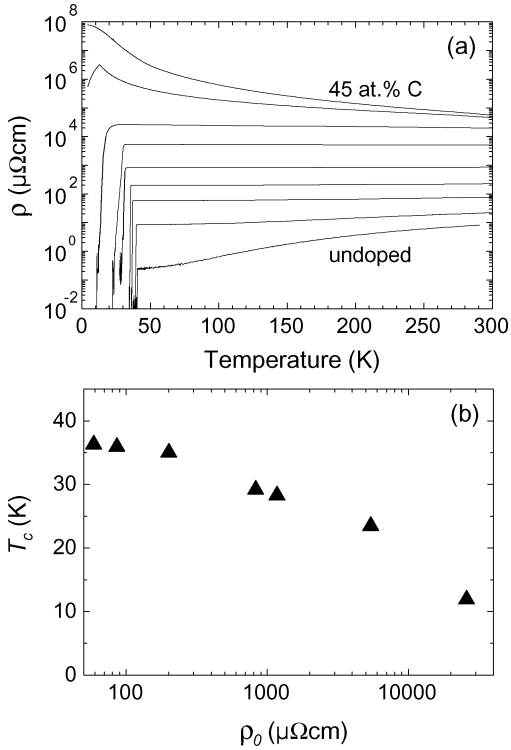

Fig. 3. (a) Resistivity versus temperature curves for MgB_2 films of different carbon doping. From bottom to top, the nominal carbon concentrations of the curves are 0, 7.4, 15, 22, 29, 34, 39, 42, and 45 at.%. (From Pogrebnyakov *et al.* [9]); (b) T_c as a function of ρ_0 for the series of carbon-doped MgB_2 films in (a).

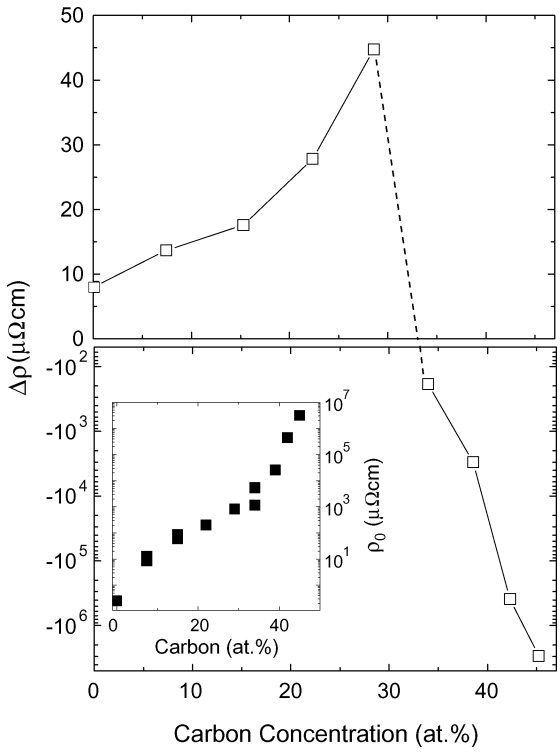

Fig. 4. Resistivity difference, $\Delta\rho \equiv \rho(300\ \mathrm{K}) - \rho(50\ \mathrm{K})$, as a function of the carbon concentration. A negative value indicates a complete blockage of the conductivity path between $Mg(B_{1-x}C_x)_2$ grains. Inset: residual resistivity as a function of carbon concentration.

at a residual resistivity of 50 $\mu\Omega\mathrm{cm}$ when 12.5 at.% of carbon is doped into MgB_2 [11]. In carbon-doped filaments, a carbon concentration of 10 at.% suppresses T_c to ~23 K [6]. Evidently, only a small portion of the carbon in the films is doped into the MgB_2 structure and the rest forms high resistance grain boundaries. Because of the complex microstructure of the carbon-doped films and the uncertainty about the amount of carbon doped into the MgB_2 structure, the residual resistivity before the superconducting transition, ρ_0, is often a better indicator of the doping level than the nominal carbon concentration in our carbon-doped HPCVD MgB_2 films. As one can see in Fig. 3(b), there is a clear correlation between T_c and ρ_0.

It has been pointed out by Rowell [12] that the resistivity of MgB_2, as reported in the literature in single crystal, polycrystalline bulk, thin film and wire samples, varies by orders of magnitude, while many high resistivity samples have T_cs near 39 K. He proposed a simple explanation that in many samples only a fraction of the cross sectional area of the sample is carrying current. Reduced density (porosity) and grain boundaries made of MgO, boron oxide, or other impurity phases can all lead to poor connectivity between the MgB_2 grains. According to the structural analysis discussed above, the Rowell model provides an ideal explanation to the properties of our carbon-doped MgB_2 films. Indeed, the resistivity of the carbon-doped films changes by orders of magnitude while the change in T_c is small.

The reduced connectivity can be measured by the temperature-dependent part of the resistivity. According to Rowell [12], the resistivity of MgB_2 samples can be fit by an expression of the form

$$\rho(T) = F\left[\Delta\rho_{sc}(T) + \rho_0\right], \quad \Delta\rho = F[\Delta\rho_{sc}], \qquad (1)$$

where $\Delta\rho_{sc}(T)$ is the temperature-dependent part of the resistivity of the single crystal, assumed to be the intrinsic property of MgB_2, $\Delta\rho \equiv \rho(300\ \mathrm{K}) - \rho(50\ \mathrm{K})$ and $\Delta\rho_{sc}$ is that of the single crystal, and $1/F$ is the fraction of the area of the sample cross section that carries current. While ρ_0 can be affected by the intragrain effects such as defects and impurities, F is a measure of the intergrain effects, or the reduced connectivity.

Fig. 4 shows $\Delta\rho$ as a function of the carbon concentration for the series of films in Fig. 3. $\Delta\rho$ increases with the carbon concentration from $\sim 8\ \mu\Omega\mathrm{cm}$ for undoped sample to $\sim 45\ \mu\Omega\mathrm{cm}$ for the carbon concentration of 29 at.%. This increase is much smaller than the increase in the residual resistivity, shown in the inset, which is about four orders of magnitude over the same doping range. As the carbon doping increases further, a negative $\Delta\rho$ is observed and the resistivity increases dramatically, indicating that the conduction path between the $Mg(B_{1-x}C_x)_2$ grains becomes completely blocked by the high resistivity grain boundaries. The carbon concentration when this occurs coincides with the x-ray diffraction result when the lattice constants of $Mg(B_{1-x}C_x)_2$ experience sudden changes.

The MgB_2 area fraction, $1/F$, is calculated following (1), using the $\Delta\rho$ value of $\sim 8\ \mu\Omega\mathrm{cm}$ for the pure MgB_2 film as $\Delta\rho_{sc}$. The result is plotted in Fig. 5 as a function of the carbon concentration before the conduction path is blocked by the grain

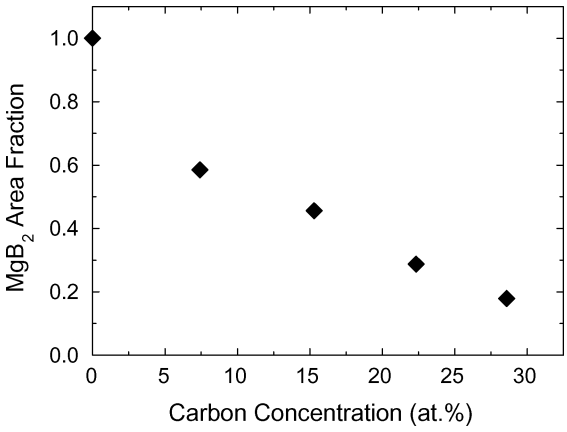

Fig. 5. MgB_2 area fraction, $1/F$, as a function of the carbon concentration.

boundaries. While the residual resistivity increases by four orders of magnitude from the pure sample to a carbon doping of $\sim$29 at.%, the conduction area between the MgB_2 grains is reduced to 20%. As pointed out by Rowell *et al.*, this reduction also affects the capability of MgB_2 samples to carry supercurrent [12], [13]. The result here is significant: while the H_{c2} of MgB_2 can be enhanced substantially by carbon doping, the negative impact of the high resistivity grain boundaries is limited. For example, a sample with $\sim$22 at.% carbon doping showed a high $H_{c2}(0)$ of $\sim$70 T [7], and its apparent J_c should be about 30% of that of $Mg(B_{1-x}C_x)_2$ without the reduced conduction area. As shown in our previous work, for carbon-doped films the self-field J_c is lower than the pure MgB_2 films, but J_c values are relatively high in much higher magnetic fields, indicating a significantly enhanced vortex pinning in carbon doped MgB_2 films [9].

V. Conclusions

Carbon-doped MgB_2 thin films were deposited by HPCVD by adding $(MeCp)_2Mg$ to the carrier gas. The degree of carbon doping can be easily controlled by the secondary H_2 flow rate through the $(MeCp)_2Mg$ bubbler. By this process, only a small portion of carbon is doped into MgB_2 and the rest is contained in the highly resistive amorphous grain boundaries. As the carbon doping increases, the high resistivity grain boundaries gradually reduces the cross section of the conduction path between the $Mg(B_{1-x}C_x)_2$ grains, leading to a rapid increase in the resistivity but a much slower decrease in T_c. Although the carbon doping significantly enhances H_{c2}, as we have reported previously [7], the reduced conduction area negatively impacts J_c. The two effects may be correlated, and a research to investigate the optimal doping condition is needed. In summary, the technique of carbon doping in HPCVD films produces MgB_2 materials that are very promising for high magnetic-field applications.

References

[1] A. Gurevich, S. Patnaik, V. Braccini, K. H. Kim, C. Mielke, X. Song, L. D. Cooley, S. D. Bu, D. M. Kim, J. H. Choi, L. J. Belenky, J. Giencke, M. K. Lee, W. Tian, X. Q. Pan, A. Siri, E. E. Hellstrom, C. B. Eom, and D. C. Larbalestier, "Very high upper critical fields in MgB_2 produced by selective tuning of impurity scattering," *Supercond. Sci. Technol.*, vol. 17, pp. 278–286, 2004.

[2] P. C. Canfield and G. Crabtree, "Magnesium diboride: Better late than never," *Phys. Today*, vol. 56, no. 3, pp. 34–40, 2003.

[3] H. J. Choi, D. Roundy, H. Sun, M. L. Cohen, and S. G. Louie, "The origin of the anomalous superconducting properties of MgB_2," *Nature (London)*, vol. 418, pp. 758–760, 2002.

[4] W. Pickett, "Mind the double gap," *Nature (London)*, vol. 418, pp. 733–734, 2002.

[5] S. Souma, Y. Machida, T. Sato, T. Takahashi, H. Matsui, S.-C. Wang, H. Ding, A. Kaminski, J. C. Campuzano, S. Sasaki, and K. Kadowaki, "The origin of multiple superconducting gaps in MgB_2," *Nature (London)*, vol. 423, pp. 65–67, 2003.

[6] R. H. T. Wilke, S. L. Bud'ko, P. C. Canfield, D. K. Finnemore, R. J. Suplinskas, and S. T. Hannahs, "Systematic effects of carbon doping on the superconducting properties of $Mg(B_{1-x}C_x)_2$," *Phys. Rev. Lett.*, vol. 92, p. 217 003, 2004.

[7] V. Braccini, A. Gurevich, J. Giencke, M. Jewell, C. B. Eom, D. C. Larbalestier, A. Pogrebnyakov, Y. Cui, B. T. Liu, Y. F. Hu, J. M. Redwing, Q. Li, X. X. Xi, R. Singh, R. Gandikota, J. Kim, B. Wilkens, N. Newmann, J. Rowell, B. Moeckly, V. Ferrando, C. Tarantini, D. Marr, M. Putti, C. Ferdeghini, R. Vaglio, and E. Haanappel, "The development of very high upper critical field in alloyed MgB_2 thin films," *Phys. Rev. B*, to be published.

[8] A. V. Pogrebnyakov, J. M. Redwing, J. E. Jones, X. X. Xi, S. Y. Xu, Q. Li, V. Vaithyanathan, and D. G. Schlom, "Thickness dependence of the properties of epitaxial MgB_2 thin films grown by hybrid physical-chemical vapor deposition," *Appl. Phys. Lett.*, vol. 82, pp. 4319–4321, 2003.

[9] A. V. Pogrebnyakov, X. X. Xi, J. M. Redwing, V. Vaithyanathan, G. Schlom, A. Soukiassian, S. B. Mi, C. L. Jia, J. E. Giencke, C. B. Eom, J. Chen, Y. F. Hu, Y. Cui, and Q. Li, "Properties of MgB_2 thin films with carbon doping," *Appl. Phys. Lett.*, vol. 85, pp. 2017–2019, 2004.

[10] X. H. Zeng, A. V. Pogrebnyakov, A. Kotcharov, J. E. Jones, X. X. Xi, E. M. Lysczek, J. M. Redwing, S. Y. Xu, Q. Li, J. Lettieri, D. G. Schlom, W. Tian, Q. Pan, and Z. K. Liu, "*In situ* epitaxial MgB_2 thin films for superconducting electronics," *Nature Mater.*, vol. 1, pp. 35–38, 2002.

[11] S. Lee, T. Masui, A. Yamamoto, H. Uchiyama, and S. Tajima, "Carbon-substituted MgB_2 single crystals," *Physica C*, vol. 397, pp. 7–13, 2003.

[12] J. Rowell, "The widely variable resistivity of MgB_2 samples," *Supercond. Sci. Tech.*, vol. 16, pp. R17–R27, 2003.

[13] J. Rowell, S. Y. Xu, X. H. Zeng, A. V. Pogrebnyakov, Q. Li, X. X. Xi, J. M. Redwing, W. Tian, and X. Pan, "Critical current density and resistivity of MgB_2 films," *Appl. Phys. Lett.*, vol. 83, pp. 102–104, 2003.